

## The General Circulation Model Response to a North Pacific SST Anomaly: Dependence on Time Scale and Pattern Polarity

YOCHANAN KUSHNIR

*Atmospheric and Oceanic Sciences Program, Princeton University, Princeton, New Jersey\**

NGAR-CHEUNG LAU

*Geophysical Fluid Dynamics Laboratory/NOAA, Princeton University, Princeton, New Jersey*

(Manuscript received 26 April 1991, in final form 6 August 1991)

### ABSTRACT

A general circulation model was integrated with perpetual January conditions and prescribed sea surface temperature (SST) anomalies in the North Pacific. A characteristic pattern with a warm region centered northeast of Hawaii and a cold region along the western seaboard of North America was alternately added to and subtracted from the climatological SST field. Long 1350-day runs, as well as short 180-day runs, each starting from different initial conditions, were performed. The results were compared to a control integration with climatological SSTs.

The model's quasi-stationary response does not exhibit a simple linear relationship with the polarity of the prescribed SST anomaly. In the short runs with a negative SST anomaly over the central ocean, a large negative height anomaly, with an equivalent barotropic vertical structure, occurs over the Gulf of Alaska. For the same SST forcing, the long run yields a different response pattern in which an anomalous high prevails over northern Canada and the Alaskan Peninsula. A significant reduction in the northward heat flux associated with baroclinic eddies and a concomitant reduction in convective heating occur along the model's Pacific storm track. In the runs with a positive SST anomaly over the central ocean, the average height response during the first 90-day period of the short runs is too weak to be significant. In the subsequent 90-day period and in the long run an equivalent barotropic low occurs downstream from the warm SST anomaly. All positive anomaly runs exhibit little change in baroclinic eddy activity or in the patterns of latent heat release. Horizontal momentum transports by baroclinic eddies appear to help sustain the quasi-stationary response in the height field regardless of the polarity of the SST anomaly. These results emphasize the important role played by baroclinic eddies in determining the quasi-stationary response to midlatitude SST anomalies. Differences between the response patterns of the short and long integrations may be relevant to future experimental design for studying air-sea interactions in the extratropics.

### 1. Introduction

The association between the seasonal sea surface temperature (SST) field in the midlatitude oceans and the long-term variability of the atmosphere has received ongoing scientific attention for the past few decades. Namias (1959, 1965, 1969, 1978) argued that large-scale anomalies in the distribution of SST in the North Pacific could interact with the regional circulation of the atmosphere on time scales ranging from weeks to months. Namias and Cayan (1981) summarized the importance of this association by drawing attention to

the spatial resemblance between the wintertime SST anomalies and regional anomalies in the geopotential height field. While these similarities may indicate that seasonal SST anomalies are being forced by the atmosphere, Namias and Cayan also suggested that they are indicative of an ocean-atmosphere feedback. The long persistence time scale of SST anomalies implies a significant change in the heat content of the wintertime oceanic mixed layer in the midlatitudes. This change, they argued, could affect the intensity of weather disturbances and the nature of the mean wintertime circulation over the adjacent oceanic area and continents. Thus, it is possible that knowledge of the SST distribution in the fall or the beginning of winter could be useful for predicting the climate of the following winter.

During winter, the leading patterns of SST anomalies in the Pacific and Atlantic basins are strongly correlated with the leading modes of variability in the sea level pressure and midtropospheric geopotential height fields

---

\* *Present affiliation:* Lamont-Doherty Geological Observatory of Columbia University.

---

*Corresponding author address:* Dr. Yochanan Kushnir, Lamont-Doherty Geological Observatory, Columbia University, Palisades, NY 10964.

(Davis 1976; Lanzante 1984; Iwasaka et al. 1987; Wallace and Jiang 1987; and Wallace et al. 1990). In one phase, the dominant pattern of Pacific SST variability is characterized by

- a large region of anomalously warm water (up to 2°C), extending from the Asian coast to 140°W between 30° and 50°N
- a belt of anomalously cold water (0.5°–1°C) along the northern and eastern rim of the ocean basin and over the subtropics.

(We shall hereafter refer to this phase of the pattern as the “warm” anomaly.)

The pressure anomaly throughout the troposphere, associated with this SST anomaly exhibit the following structure:

- a high south of the Aleutians (roughly over the center of the SST anomaly)
- a trough extending from the subtropics to the western United States and Canada
- a high over the southeastern United States.

This pattern is similar to the Pacific/North American (PNA) pattern of Wallace and Gutzler (1981). In the opposite phase of the SST anomaly, the polarity of the geopotential height anomaly is reversed.

The possible effect of anomalous SST forcing on the atmosphere was studied by Hoskins and Karoly (1981), Hendon and Hartmann (1982), and Held (1983) using linear, stationary-wave models. These studies assumed that a warm (cold) extratropical SST anomaly introduces a shallow heat source (sink) in the lower troposphere. Linear, quasigeostrophic considerations require the heating anomaly to be balanced by horizontal temperature advection. Meridional advection of the mean temperature field is accomplished by a surface low pressure anomaly that forms downstream of the warm water. The mean zonal wind contributes to the thermal balance by advecting air from a shallow cold anomaly located upstream of the warm water. The phase relationship between the surface pressure and temperature perturbations requires the phase lines of the geopotential height anomaly to tilt westward with increasing height. This relationship was verified in models with a full spherical geometry. It is notable, however, that the prescribed heating anomalies needed to generate a reasonable atmospheric response in these models are about 10°C day<sup>-1</sup>. These results are not consistent with the observed relationships described in the preceding paragraph. Frankignoul (1985) noted these discrepancies in a review of theoretical and modeling work pertaining to the understanding of midlatitude ocean–atmosphere interactions. He attributed the difficulties in simulating the response to SST anomalies to the uncertainties in the relationship between the latter and the distribution of the sources and sinks of heat in the atmosphere.

Recent GCM experiments with prescribed midlatitude SST anomalies were more successful than linear models in simulating the observed SST–geopotential height relationship. Palmer and Sun (1985) investigated the response to North Atlantic SST anomalies by using the U.K. Meteorological Office GCM. They integrated the model four times, each for a period of 50 days, with negative and positive SST anomalies of up to 3°C, and examined the linear part of the response (e.g., the difference between the warm and cold runs). Their analysis yielded a realistic relationship, with a positive and equivalent barotropic height anomaly being simulated somewhat downstream of the warm water surface. Pitcher et al. (1988) forced the NCAR Community Climate Model (CCM) with a realistic Pacific SST anomaly in a long integration with perpetual January conditions. From the data generated in those experiments, they formed two ensembles of eight independent realizations of 90-day averages. They separately compared the “cold” and “warm” anomaly ensembles to a control integration of similar length. They found a significant response to cold SSTs in the form of a PNA pattern with a low south of the Aleutians. Surprisingly, however, the atmospheric response to the warm anomaly was quite similar to the response to the cold one. Most recently, Lau and Nath (1990) integrated the GFDL GCM for an interval of 30 years with the SSTs prescribed to vary in a realistic manner over almost the entire World Ocean (including the tropics). Observations of monthly mean SST anomalies from 1950 to 1979 were used to provide the lower boundary forcing. Lau and Nath diagnosed the relationship between the SST field and different atmospheric variables using linear statistical techniques such as principal component analysis and correlations, in a way similar to Wallace et al. (1990). They reported that during winter, realistic relationships were simulated between the SST fields of the North Pacific and North Atlantic oceans and the Northern Hemisphere atmospheric circulation.

In their GCM studies, both Palmer and Sun (1985) and Lau and Nath (1990) made a special effort to diagnose the dynamical effects of baroclinic eddies. Examining the baroclinic eddy fluxes of momentum and heat, they found that the perturbations in the SST field were associated with significant shifts in the positions of the storm tracks. The changes in momentum fluxes produced sources and sinks of vorticity, consistent with the anomalies in the seasonal circulation. Palmer and Sun also argued that the eddy vertical heat fluxes substantially modify the midlatitude troposphere, by effectively deepening the heat sources in the atmosphere. Lau and Nath noted the changes in the patterns of precipitation due to the displacement of the storm tracks. These changes caused the redistribution of the sources and sinks of heat in their experiment and may have contributed to the changes in the mean circulation.

The importance of baroclinic eddies in shaping the long-term atmospheric response to midlatitude SSTs was also noted in an idealized GCM experiment by Ting (1991). In this nonlinear model, full parameterization of the physical processes was incorporated, but the model included no continents or orography. The model was integrated with fixed positive and negative SST anomalies in the midlatitudes, each integration lasting for 2000 days. The convergence patterns of heat transport by the baroclinic eddies were modified by the anomalous SST distribution. The field of convective heating was also modified as a result of the changes in baroclinic eddy activity. However, the simulated geopotential height response was similar to the results of linear, stationary wave models, and not to observations. Here too a large SST anomaly of 10 K had to be specified in order to obtain a response with a reasonable amplitude. Ting carefully analyzed her results using a linearized version of her model. She showed that the reasons for the similarity to linear model studies were that the eddies in the idealized GCM acted as simple diffusive mechanisms in the thermodynamic equation. Sensible heating in her model had the net effect of simple Newtonian damping, and latent heat release was closely related to the evaporation anomaly and the SST anomaly. Such behavior is quite similar to the manner in which the eddy effects were parameterized in the studies of Hoskins and Karoly (1981) and Hendon and Hartmann (1982). Thus, the study by Ting appears to imply that models in which the unperturbed climate is zonally symmetric do not exhibit a realistic response to SST anomalies.

In the present study, we sought to reconcile the differences in the GCM experiments described in the preceding paragraphs and to understand further the role of baroclinic eddies in midlatitude ocean-atmosphere interactions. In view of the seemingly important role of zonal asymmetries in these interactions, we planned to integrate a full GCM. The model used by Lau and Nath (1990) was adapted for the present study. To simplify the experimental setting, the model was forced with a realistic but time-independent SST anomaly and integrated with perpetual January conditions. Long continuous integrations (like those of Pitcher et al. 1988 and Ting 1990) were conducted to obtain what may be referred to as the model "equilibrium" response. The "transient" effects in the experiments of Palmer and Sun (1985) and Lau and Nath (1990) were simulated by several relatively short runs, each starting from different initial conditions. Positive and negative anomaly ensembles were created by alternating the polarity of the SST anomaly. Each ensemble was compared to an unperturbed "control" run. The details of the experimental design are described in section 2. The results are presented in section 3 in terms of the geopotential height response, the baroclinic eddy statistics, and the structure of the diabatic heating fields. Summary and discussion follow in section 4.

## 2. Methodology

### a. The model

The simulations were performed using a spectral GCM with rhomboidal truncation at wavenumber 15 (corresponding to a  $4.5^\circ$  latitude by  $7.5^\circ$  longitude grid). This model has nine unequally spaced "sigma" levels in the vertical. The model was developed at the NOAA Geophysical Fluid Dynamics Laboratory (GFDL) and is maintained by the Climate Dynamics Project there. The model physics include moist convective adjustment and bulk aerodynamics to calculate the momentum, heat, and moisture transfer from the surface to the atmosphere. Also included is a radiative transfer scheme that uses fixed, zonally symmetric clouds from the observed climatology. SST and sea ice are prescribed. In all these details, the model is identical to that used by Lau and Nath (1990). In this study however, the model was integrated with "perpetual" January conditions, that is, with the solar zenith angle fixed at its mid-January value, and surface boundary conditions fixed at their typical January distributions. To determine the soil moisture content and snow depth, the January climatology of a previous 10-year model integration, which incorporated the seasonal cycle, was used. With these conditions set, a "control" integration was performed, starting from a previously archived January state and extending for 1350 days. During the control integration the SST field was prescribed using the January climatology. The control integration produced a stable climatology. Compared to a previous model run that incorporated the seasonal cycle, the westerly jet over the northern midlatitudes was stronger and shifted somewhat northward. This was most notable in the upper troposphere and is consistent with a colder upper troposphere, due perhaps to extended radiative cooling in the polar night region.

### b. The experiments

The SST anomaly used in this study (Fig. 1) is based on the regression pattern between the first rotated principal component of North Pacific SST and the total SST field (see Lau and Nath 1990, Fig. 13a). When added to the climatology, it served as boundary conditions for the positive anomaly runs. The negative anomaly experiments were integrated with the same anomaly subtracted from the climatological mean SST field. The pattern exhibits a dipole with centers of action over the eastern ocean basin. It resembles the first EOF of North Pacific SST in Davis (1976, Fig. 4) and the second nonseasonal pattern in Weare et al. (1976, Fig. 8). The regression pattern was scaled up to a maximum of  $2^\circ\text{C}$  at  $40^\circ\text{N}$ ,  $150^\circ\text{W}$  and a minimum of  $-1.4^\circ\text{C}$  at  $35^\circ\text{N}$ ,  $125^\circ\text{W}$ . With this scaling the pattern represents a realistic, though somewhat strong, anomaly, as can be seen by examining the atlas compiled by

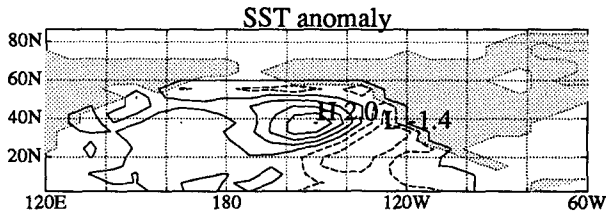


FIG. 1. The anomaly pattern in the SST field in its "positive" polarity. Contour interval is 0.5°C, negative contours are dashed.

Namias (1979). In ocean areas outside the North Pacific, the anomaly values were set to zero.

In order to distinguish between the relatively short-term model response and the equilibrium one, similar SST anomalies were specified in two types of integrations: long integrations similar to the control run and short 180-day integrations, each starting from different initial conditions. Two long integrations were performed, one with the anomaly in its positive polarity and the other with the polarity of the anomaly reversed. Eight pairs of "short" anomaly runs were performed, using initial conditions taken at 90-day intervals from the control, with each pair containing a positive and a negative case.

### c. Determining the model response

The quasi-stationary model response to the SST anomaly was determined by calculating long-term time averages from the model's daily output. For the purpose of evaluating the robustness of the results, we have divided the output of the long runs (control and anomaly) into statistically independent segments. This was done, as in Pitcher et al. (1988), by calculated non-overlapping 90-day averages separated by 60-day intervals, beginning on day 61 of the long model integration (i.e., the average of day 61–150 was followed by the average of day 211–300, etc.). The control ensembles will hereafter be referred to as CN. The anomaly ensembles will be referred to as the "long positive" (LP) and "long negative" (LN) runs, respectively. The data records output from each of the short runs were considered statistically independent from one another by virtue of their being started from different initial conditions. Four ensembles of 90-day averages were derived from the short runs. The first 90-day period (day 1–90) of the short runs will hereafter be referred to as "short positive" (SP) and "short negative" (SN) ensembles, respectively. The second 90-day period (day 91–180) of the short runs will be referred to as the "extended positive" (EP) and "extended negative" (EN) ensembles. The initial 180-day period of the two long experiments was processed in a manner similar to the short runs, bringing the total number of independent realizations in each of the SP, SN, EP, and EN ensembles to nine. Eddy covariances statistics, representing 90-day averages of fluxes in the 2–10-day

band, were calculated from the model's daily output by means of a bandpass filter similar to that used by Lorenz (1979).

The model sensitivity to the change in SST distribution was investigated by calculating the differences between the anomaly and the control ensembles at each model grid point. The statistical significance of the results was assessed on the basis of simple hypothesis testing of the local differences. We used the two-sided Student's *t*-test (e.g., Morrison 1976). In the present study, *t* statistics were calculated as described in Pitcher et al. (1988), with a total of 16 degrees of freedom in each comparison of anomaly versus control.

## 3. Results

In the following, attention is focused to a sector of the model grid extending from equator to pole and from 120°E eastward to 60°W. The long-term distribution of the 515-mb height deviation from the zonal mean (stationary waves) and the total 990-mb height field are shown in the upper and middle panels of Fig. 2, respectively. The model reproduces the observed location of the wintertime troughs and ridges in the mid-troposphere, as well as those of the centers of high and low geopotential near the surface (compare, e.g., Trenberth and Olson 1988, Fig. 25). Over North America the stationary wave amplitude at the 515-mb level is weaker than observed. The model's zonally averaged tropospheric jet (not shown) is weaker than observed. The surface westerlies, however, are stronger than observed by a factor of 1.5 to 2. The bottom panel of Fig. 2 shows the mean control distribution of northward eddy heat flux in the 2–10-day band. The model has an unrealistic storm track, centered over Alaska rather than over the central North Pacific.<sup>1</sup> Thus, the main center of the SST anomaly dipole is located just south of a region of maximum baroclinic activity. The relative location of the storm track and the SST anomaly dipole may be important in determining the transient eddy response, as will be discussed later in sections 3b and 4.

### a. Geopotential height response

The ensemble mean 990- and 515-mb height differences between the perturbed SST runs and the control integration are shown in Figs. 3 and 4. The left panels are for the positive anomaly runs, and the right panels for the negative anomaly ones. The top panels are for the first 90-day period of the short runs (SP and SN), the middle panels are for the second 90-day period of the short runs (EP and EN), and the bottom panels

<sup>1</sup> This unrealistic feature is not present in a previous version of this GCM (Lau and Nath 1987, Fig. 1f) but is discernable from the output of a recent 100-year integration of a current version of the model.

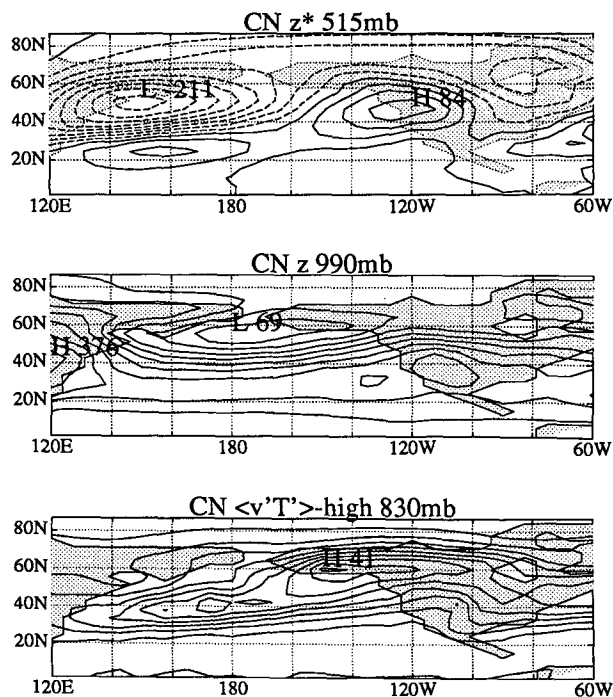


FIG. 2. The model's long-term mean geopotential height deviation from the zonal mean at 515 mb (top), total geopotential height field at 990 mb (middle), and baroclinic eddy northward heat flux (bottom). Contour interval is 25 m, 30 m, and  $5^{\circ}\text{C m s}^{-1}$ , respectively; negative contours are dashed.

are for the long integrations (LP and LN). The regions where the height differences exceed the 95% levels of significance, according to a univariate two sided  $t$ -variable, are depicted by dark shading.

The initial response to a positive SST anomaly (SP, Figs. 3, 4, upper left panel) is weak and may not be significantly different from zero. The sense of the response in the vicinity of the warm SST center is nevertheless the same as the clear coherent signal in the subsequent 90-day period (EP, Figs. 3 and 4, middle left panel) and in the long run (LP, Figs. 3 and 4, bottom left panel). In the midlatitudes the response exhibits an equivalent barotropic vertical structure. (The 205-mb response, not shown, is identical in phase and somewhat stronger than the 515-mb response.) Over the eastern subtropical Pacific (a region of anomalously cold water), the low-level response is characterized by a small amplitude but significant positive height anomaly (Fig. 3, left panels). Overlying this low-level feature is a weak negative height anomaly in the upper troposphere (Fig. 4, left panels), indicating the presence of a baroclinic response in the subtropics.

In contrast to the positive anomaly runs, the first 90 days of the short negative runs (SN, Figs. 3 and 4, upper right panels) exhibit a coherent and large-amplitude negative height anomaly over the Gulf of Alaska. The level of statistical significance of this re-

sponse is high. This negative anomaly has an equivalent barotropic vertical structure. (The 205-mb response, not shown, is in phase and almost identical to the 515-mb response.) In the subsequent 90-day period (EN, Figs. 3 and 4, middle right panels), the negative height anomaly appears to be displaced eastward, and a positive height anomaly emerges over northern Canada. Both the SN and EN midtropospheric response patterns (Fig. 4, right panels) exhibit a small-amplitude positive height anomaly over the subtropics. Note the resemblance between the short-term response patterns and the regression pattern of Lau and Nath (1990, Fig. 12). In the equilibrium run (LN, Figs. 3 and 4, bottom right panels), a positive height anomaly over Alaska dominates the response pattern. The negative height anomaly east of the center of the anomalous cold SST region is weaker than during the short runs, but nonetheless significant at the 95% level and above.

Overall, the patterns shown in Figs. 3 and 4 exhibit some degree of similarity, irrespective of the mode of integration or the polarity of the SST anomaly. In all panels, a low pressure anomaly is found in the vicinity of the midoceanic center of the anomalous SST dipole. A small-amplitude low pressure anomaly tends to extend eastward from this center, toward the North American continent. Such a resemblance was noted also by Pitcher et al. (1988).

In all experiments, the most prominent features in the temperature response field (not shown) are consistent with the equivalent barotropic structure of the height anomalies, that is, they are of the same polarity and in phase with the anomalies in the height field. The temperature response in the lower troposphere implies reduced baroclinicity over the northern rim of the Pacific, particularly in the negative anomaly runs.

#### b. Baroclinic eddy fluxes

Palmer and Sun (1985) and Lau and Nath (1990) suggested that the changes in the baroclinic eddy activity and in the eddy forcing of the quasi-stationary flow are crucial elements of ocean-atmosphere interactions in the midlatitudes. This hypothesis is supported by the apparent changes in the eddy fields of the present experiments. The northward eddy heat flux ( $\overline{v'T'}$ ) in the 2–10-day band (a proxy for baroclinic eddy activity) is shown in Fig. 5. The negative anomaly runs (right panels) exhibit a striking decrease in baroclinic eddy activity over the northern rim of the Pacific, Alaska, and Canada. This region coincides with the axis of the model's "climatological" storm track (Fig. 2, bottom panel). The changes in the positive runs (left panels) are weaker in amplitude and smaller in scale. Thus, while the geopotential height response to the positive and negative SST anomaly exhibit some similarities (Figs. 3 and 4), the response in baroclinic eddy activity is sensitive to the polarity of the anomaly.

The response in eddy northward heat flux varies

## Z 990 mb

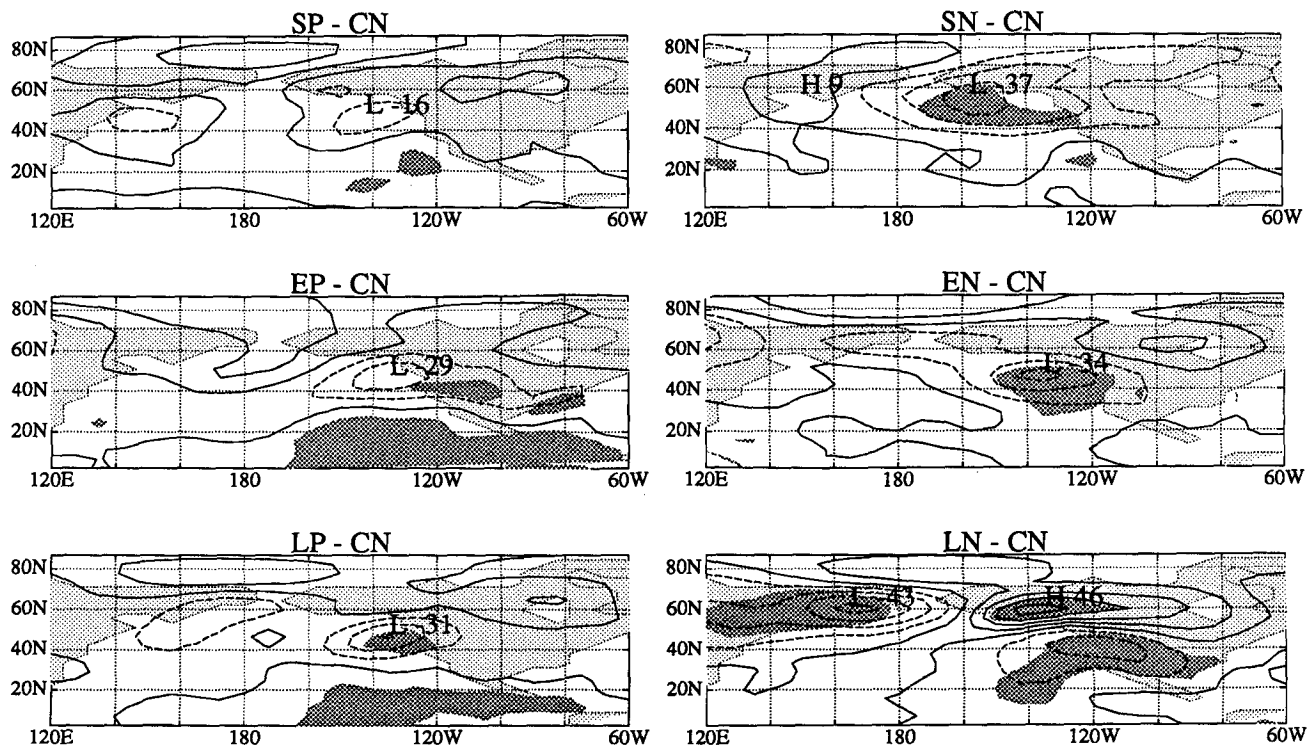


FIG. 3. The 990-mb geopotential height response (experiment – control) in the positive anomaly runs (left panels) and negative anomaly runs (right panels). Upper two panels are for the ensemble of nine averages over days 1–90 of the short anomaly runs. Middle panels are for the ensemble of nine averages of days 91–180 of the short anomaly runs. Bottom panels are for the ensemble of nine independent realizations of 90-day averages drawn from the long runs. Contour interval is 10 m, negative contours are dashed. Very light shading indicates the model continents, while the dark shading indicates regions where the response is significant above the 95% level, according to a univariate  $t$  variable calculated locally at each grid point.

somewhat from one negative anomaly experiment to another. In SN (Fig. 5, upper right panel) the attenuation in eddy activity is limited in magnitude and areal coverage. In EN (Fig. 5, middle right panel) the response pattern is larger in scale and more coherent. In LN (Fig. 5, bottom right panel) the response is stronger and more widespread than in the short runs. The changes in baroclinic eddy activity are consistent with the reduction in the baroclinicity of the quasi-stationary flow over the Pacific storm track. The surface temperature fields of the SN, EN, and LN ensembles (not shown) are all characterized by reduced meridional temperature gradients south of Alaska. This is associated not only with the prescribed anomaly in SSTs, but also with the anomalous warming over Alaska related to the anticyclonic anomaly there (see right panels of Figs. 3 and 4).

An east–west cross section through the high-latitude storm track (Fig. 6) shows that the anomaly in the eddy vertical heat flux ( $\overline{\omega'T'}$ ) reaches a maximum (i.e., exhibits the largest reduction in the upward heat transport) at the 830-mb pressure level. In the negative

anomaly runs, the vertical heat flux anomalies occur just north of the center of the negative SST anomaly. The vertical heat flux anomalies are weak in the initial 90-day period of the short runs (see SN) and intensify as the integration progresses (see EN). The response in the equilibrium run is equally strong. The changes in the vertical eddy heat flux act to warm the lower troposphere below 830 mb and cool the upper tropospheric level. In the positive anomaly runs (left panels) the positive anomalies in the vertical eddy heat flux are relatively weak.

Palmer and Sun (1985) and Lau and Nath (1990) presented evidence that eddy momentum fluxes act to reinforce the quasi-stationary geopotential height response. To examine this effect in the present study, we calculated the vertically integrated tendency in the geopotential height field due to the anomalous transport of momentum by high-frequency eddies. The height tendency was calculated using the approximation suggested by Lau (1988). This procedure entails the calculation of the convergence of eddy vorticity fluxes from the zonal and meridional eddy transport

## Z 515 mb

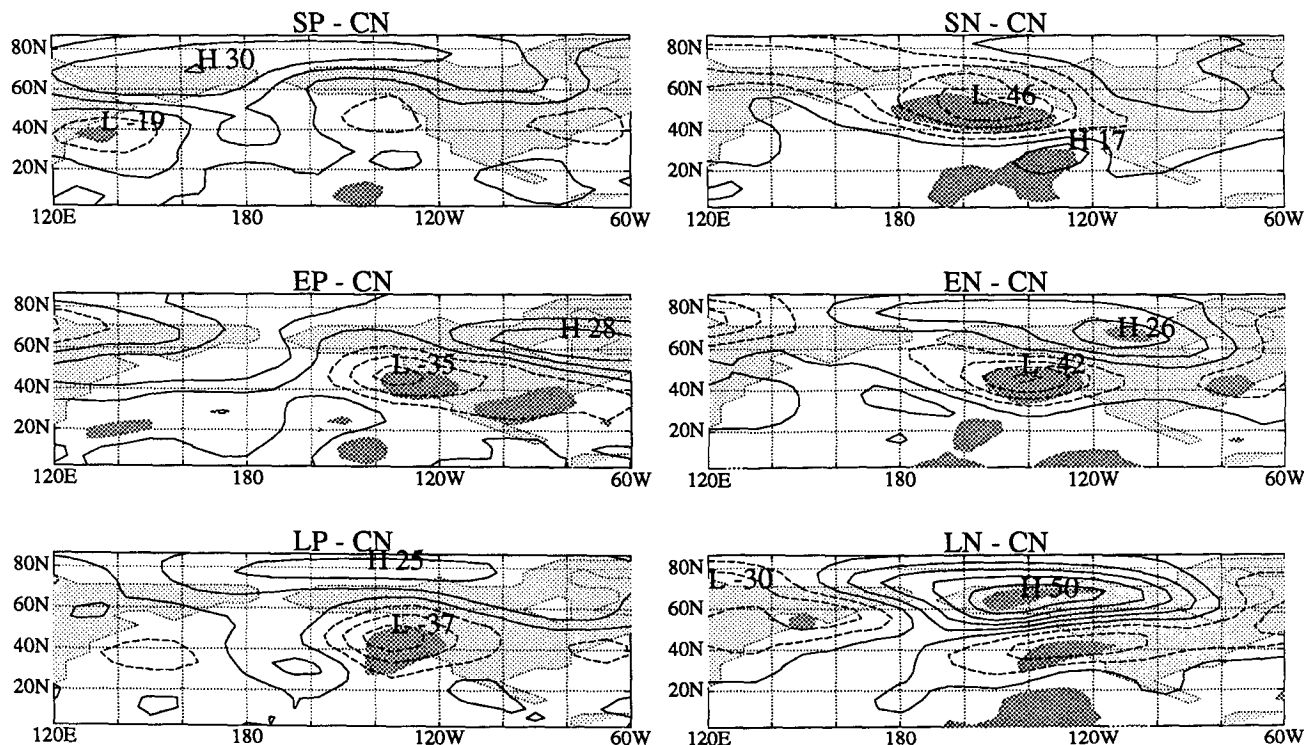


FIG. 4. As in Fig. 3, but for the response at 515 mb. Contour interval is 10 m.

of momentum (or eddy wind covariances). Using quasigeostrophic approximations, the inverse Laplacian of the convergence is proportional to the tendency of the geopotential height field (see also Lau and Nath 1990). In the present study, the eddy momentum transports were vertically integrated between 990 and 205 mb. These quantities were then used to calculate the vorticity fluxes, and subsequently, the geopotential height tendency. The results, shown in Fig. 7, indicate that the eddies tend to reinforce the quasi-stationary height anomalies (cf. Fig. 4). The effect is most coherent and significant in the short, negative anomaly runs (SN, upper right panel). Note however that the features in the height tendency field are shifted upstream with respect to the corresponding features in the geopotential height field. This shift may indicate that in the total vorticity balance the eddies tend to retard the eastward advection of the anomalous large-scale features by the underlying zonal current.

### c. The diabatic heating anomalies

The response in the vertically integrated sensible and condensational heating fields is shown in Figs. 8 and 9, respectively. In the positive anomaly runs (left panels), sensible heating dominates. A positive center is

located in almost exact phase with the warm SST anomaly at 40°N, 150°W. A weaker negative anomaly is found over the cold water to the southeast. The condensational heating field (Fig. 9) is rather noisy, but acts to enhance the sensible warming over the center of the warm SST anomaly by up to  $10 \text{ W m}^{-2}$ . The intensity of the sensible heating anomaly over the centers of the SST dipole changes very little from the initial response to the equilibrium one. All positive anomaly runs exhibit anomalous cooling, due mainly to sensible heat flux at the ocean-continent boundary in the vicinity of 60°N and the date line. This cooling is in phase with the anomalous cold ocean surface there (see Fig. 1). The vertical structure of the heating field is rather shallow, confined to the model layers below 830 mb (not shown). Thus, to first order, the response in the heating fields in the positive anomaly runs is in agreement with the results presented by Ting (1991).

The negative anomaly runs (Figs. 8 and 9, right panels) exhibit a more complex response to the SST anomaly. The magnitude of the sensible cooling over the main center of the SST anomaly is half as strong as the heating in the positive anomaly runs. This cooling is due to reduced sensible heat flux over the anomalously cold water. More prominent than the response over the center of the negative SST anomaly are the

$$\overline{v'T'}_{\text{high}} \text{ 830 mb}$$

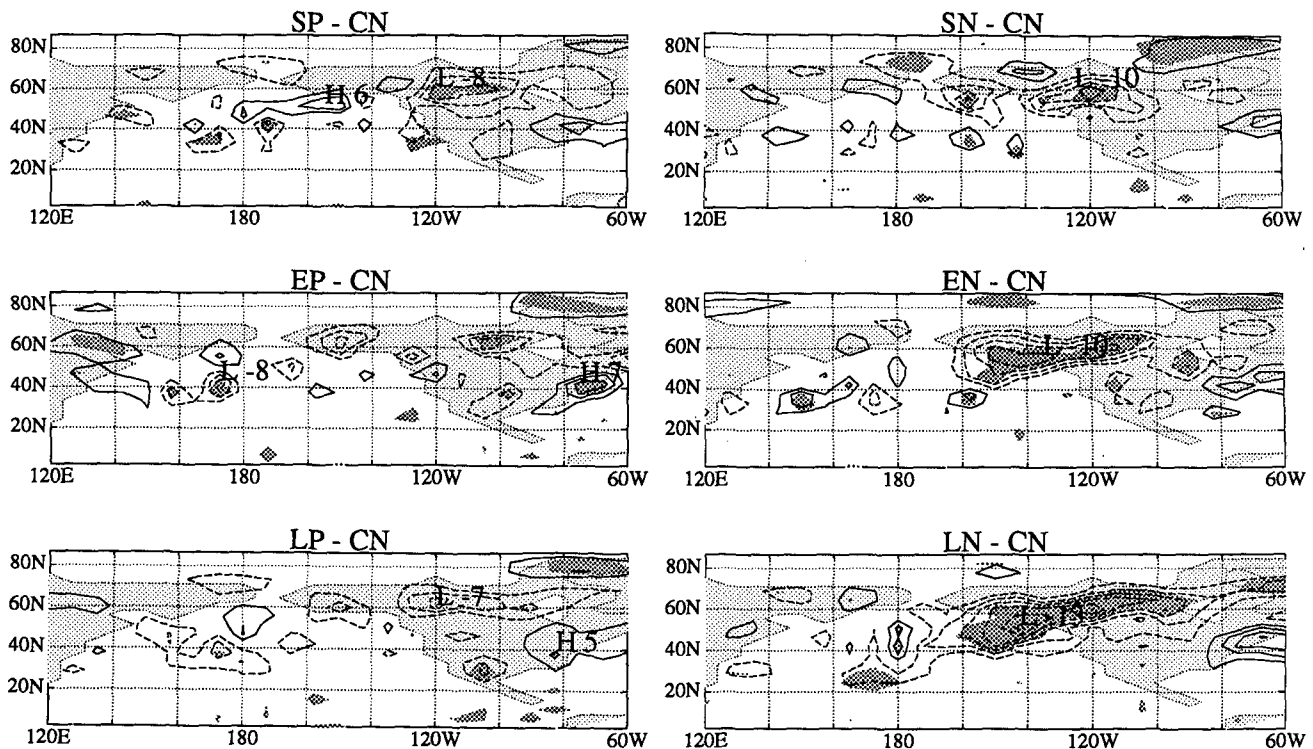


FIG. 5. As in Fig. 3, but for the northward flux of heat in the baroclinic eddy frequency band (periods of 2–10 days) at 830 mb. Contour interval is  $2^{\circ}\text{C m s}^{-1}$ , zero contour is omitted.

changes along the northern rim of the Pacific. In SN (Fig. 8, upper right panel) there is a large positive anomaly at  $\sim 60^{\circ}\text{N}$  and the date line. This anomaly is in phase with the anomalously warm water there and the northerly flow associated with the negative height anomaly over the Gulf of Alaska (Fig. 3, upper right panel). Under these conditions cold air from the snow-covered continent and frozen ocean surface to the north is being advected over the warmer water. This increases the amount of sensible heat extracted from the ocean surface, thus inducing the anomalous warming of the lower troposphere. In contrast, the equilibrium response (LN, Fig. 8, bottom right) exhibits a sensible cooling anomaly over the same location. The cooling is consistent with the change in the low-level circulation there (Fig. 3, lower right panel). The strong cell of anomalous high pressure over Alaska advects warm air from the south toward the Bering Sea, thus causing a reduction in the sensible heat flux from the ocean surface.

The midlatitude features in the condensational heating field of the negative anomaly runs (Fig. 9, right panels) occur over the Gulf of Alaska and the North American seaboard between  $30^{\circ}$  and  $40^{\circ}\text{N}$ . The increased precipitation over the western seaboard of the

United States may be due to the quasi-stationary westerly wind anomaly there (Figs. 3, 4, right panels). The negative anomalies to the north of the cold water are consistent with changes in baroclinic eddy activity there (Fig. 5, right panels), indicating that the reduction in eddy activity causes a decrease in precipitation. The anomalous cooling due to the reduced level of condensation is confined to the lowest tropospheric levels (not shown). The reduction in the vertical eddy heat flux over the storm tracks, noted earlier in section 3b (see also Fig. 5, right panels), acts to balance this anomalous condensational heat sink and cool the upper atmosphere. The differences in the intensity and spatial coverage of the convective heating anomalies in the Gulf of Alaska in SN, EN, and LN are consistent with the respective differences in the baroclinic eddy transport of heat there (Fig. 5, right panels). Thus, as noted also by Lau and Nath (1990), part of the changes in the patterns of latent heating in the anomaly runs appears to be due to changes in baroclinic eddy activity. In this way the eddies provide yet another mechanism by which they influence the quasi-stationary flow (similar arguments, but with regard to the forcing of the climatological mean flow, were made by Valdez and Hoskins 1989).



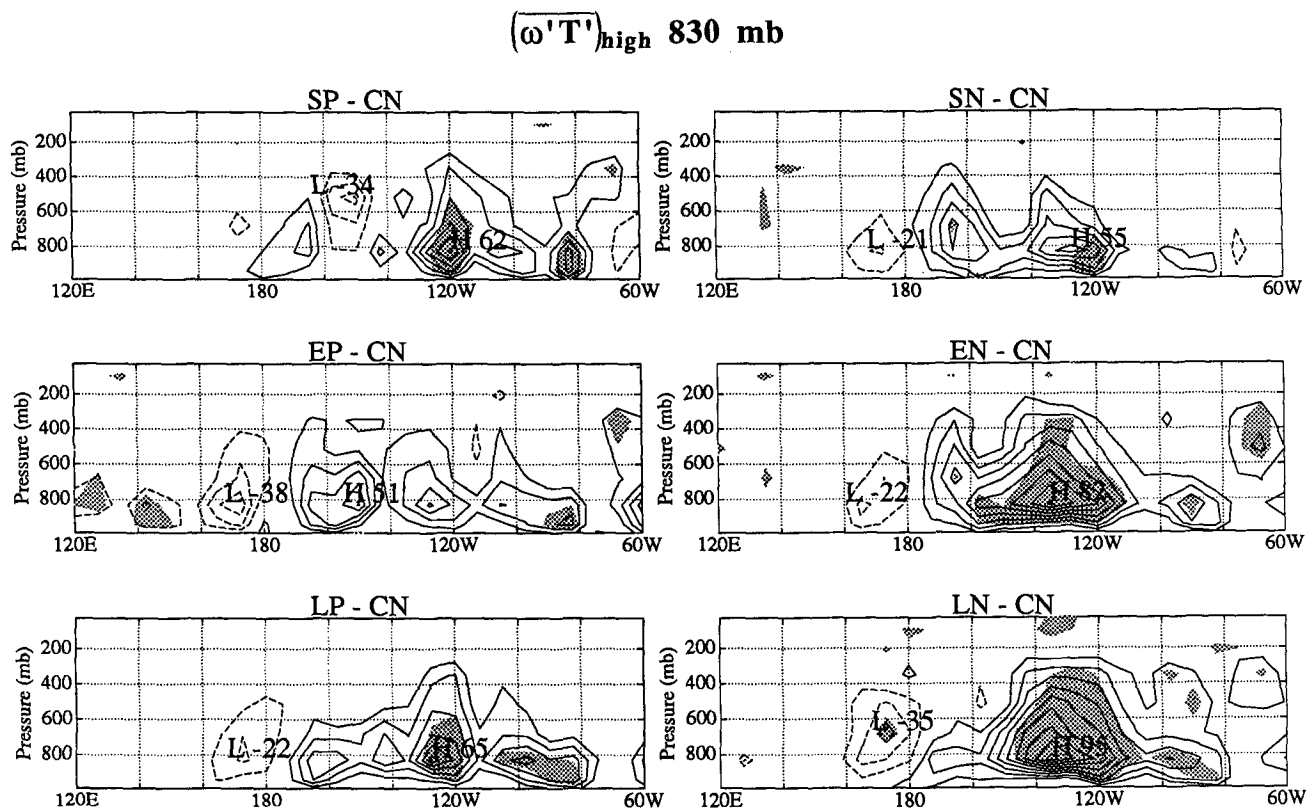


FIG. 6. Vertical cross section of the vertical heat transport in the 2–10-day band, averaged between 56° and 65°N. Panels arranged as in Fig. 3. Statistical significance levels shaded as in Fig. 3. Contour interval is 10 mb °C day<sup>-1</sup>, negative contours are dashed, zero contour is omitted.

#### 4. Summary and discussion

In the present study, the response of an atmospheric GCM to a prescribed SST distribution was examined in an attempt to improve our understanding of ocean-atmosphere interaction on seasonal time scales. Notably, the feedback between the ocean and the atmosphere, crucial to the complete understanding of the problem, was ignored. However, our intention was to simplify the problem in order to isolate and study atmospheric mechanisms that could play a role in the complete interaction.

The present GCM experiments confirm many of the results obtained in the earlier studies of Palmer and Sun (1985), Pitcher et al. (1988), and Lau and Nath (1990). They suggest that persistent regional anomalies in the midlatitude SST field can modify the wintertime circulation over the Northern Hemisphere. These modifications include changes in baroclinic eddy activity, which in turn feed back on the quasi-stationary flow through eddy flux convergences as well as eddy-induced changes in the convective and (possibly) sensible heating fields. The response patterns of these full GCMs compare more favorably with observations than the results of linear model integrations (e.g., Hoskins

and Karoly 1981; Hendon and Hartmann 1982), the response patterns of models that do not include zonal asymmetries (Ting 1991), or the effects of transient eddies (Navarra 1990). These findings suggest that both transients and zonal asymmetries are important mechanisms in the atmospheric response to midlatitude SST anomalies. However, these general statements should be scrutinized in light of the perplexing elements in the present results: namely, the similarity between the responses to negative and positive SST anomalies, the dissimilar response patterns in the baroclinic eddy heat flux fields, and the differences between initial and equilibrium response patterns. It is also notable that the response in the geopotential height field is weaker than suggested by observations. This could possibly be explained by the relatively strong surface winds found in the model simulation as argued by Held and Ting (1990) based on linear considerations, which emphasize the role of horizontal advection (see the Introduction).

The asymmetry in the response with respect to the polarity of the SST anomaly pattern was noted earlier by Pitcher et al. (1988). Pitcher et al. also noted subtle differences between the heating anomalies in their positive and negative runs. These differences seem to be

$$\left(\frac{\partial Z}{\partial t}\right)_{\text{high}}$$

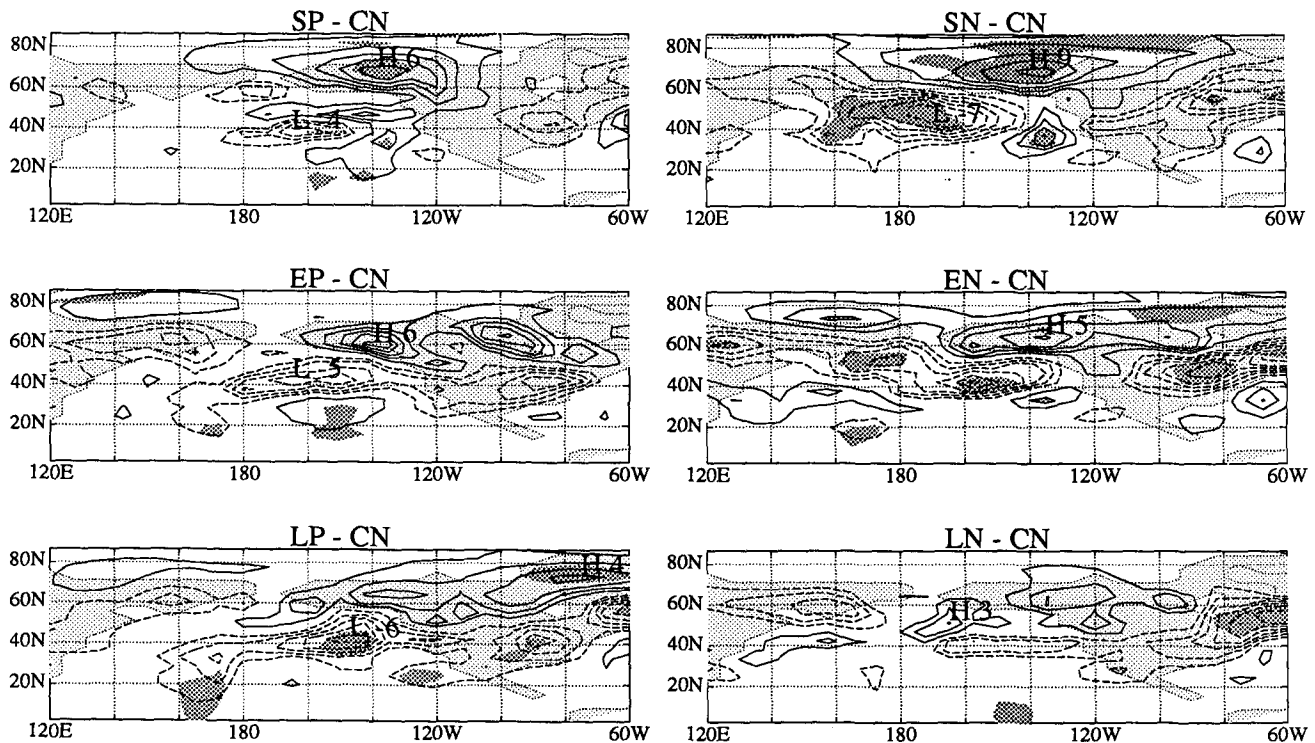


FIG. 7. As in Fig. 3, but for the 90-day averaged geopotential height tendency due to the vorticity fluxes by the 2–10-day band eddies integrated between 990 and 205 mb. Contour interval is  $1 \text{ m day}^{-1}$ ; zero contour is omitted.

rather large in our experiment. We also found that the differences in the response to the positive and negative SST anomalies are closely associated with significant differences in the response patterns of baroclinic eddy fields. In the positive SST anomaly runs little significant change occurred in the three-dimensional structure of the eddy heat flux, while the corresponding changes in the negative anomaly runs are large. Rough estimates reveal that the nature of the heat balance in the vicinity of the SST dipole depends on the sign of the SST anomaly. In the positive anomaly run, LP, cold advection of the mean temperature field by the anomalous northerlies west of the midlatitude low (ranging from  $-0.4^\circ$  to  $-0.8^\circ \text{C day}^{-1}$ ) could balance the sensible heating anomaly found over the warm water. In contrast, the negative anomaly run, LN, exhibits an increased eddy heat flux convergence over the cold water due to reduced northward eddy heat flux over the Gulf of Alaska. This increased convergence (about  $0.4^\circ$  to  $0.6^\circ \text{C day}^{-1}$ ) could balance the anomalous sensible cooling found over the cold water. In the negative anomaly runs the changes in baroclinic activity are accompanied by a source of diabatic forcing through the release of latent heat, which is larger than the direct

effect of the SST anomaly. The eddies themselves act to partially balance the convective heating deficit over the Gulf of Alaska (Fig. 9, right panels). By transporting less heat upward in the LN case (Fig. 6, bottom right), for example, baroclinic eddies induce an average anomalous warming of about  $0.5^\circ \text{C day}^{-1}$  below 800 mb, where the anomalous convective cooling is strongest (not shown). Thus, the combined effect of the eddies is to create vertically “deep” forcing in the thermodynamic balance of the quasi-stationary flow, as suggested by Palmer and Sun (1985). Note, however, that this effect does not coincide with the center of the SST anomaly in the central ocean basin.

The reasons for the lack of response in thermal transients in the positive anomaly runs are not clear. The peculiar arrangement of the Pacific storm track in the model, noted earlier (Fig. 2, bottom panel), may be responsible for this discrepancy. Initially, the prescribed SST anomaly introduces a change in the north–south gradient of surface temperature over the northern rim of the Pacific. In the negative anomaly runs, the baroclinicity there is reduced, while in the positive runs it is enhanced. It may well be that the reduction in baroclinicity has an immediate, and large, negative effect

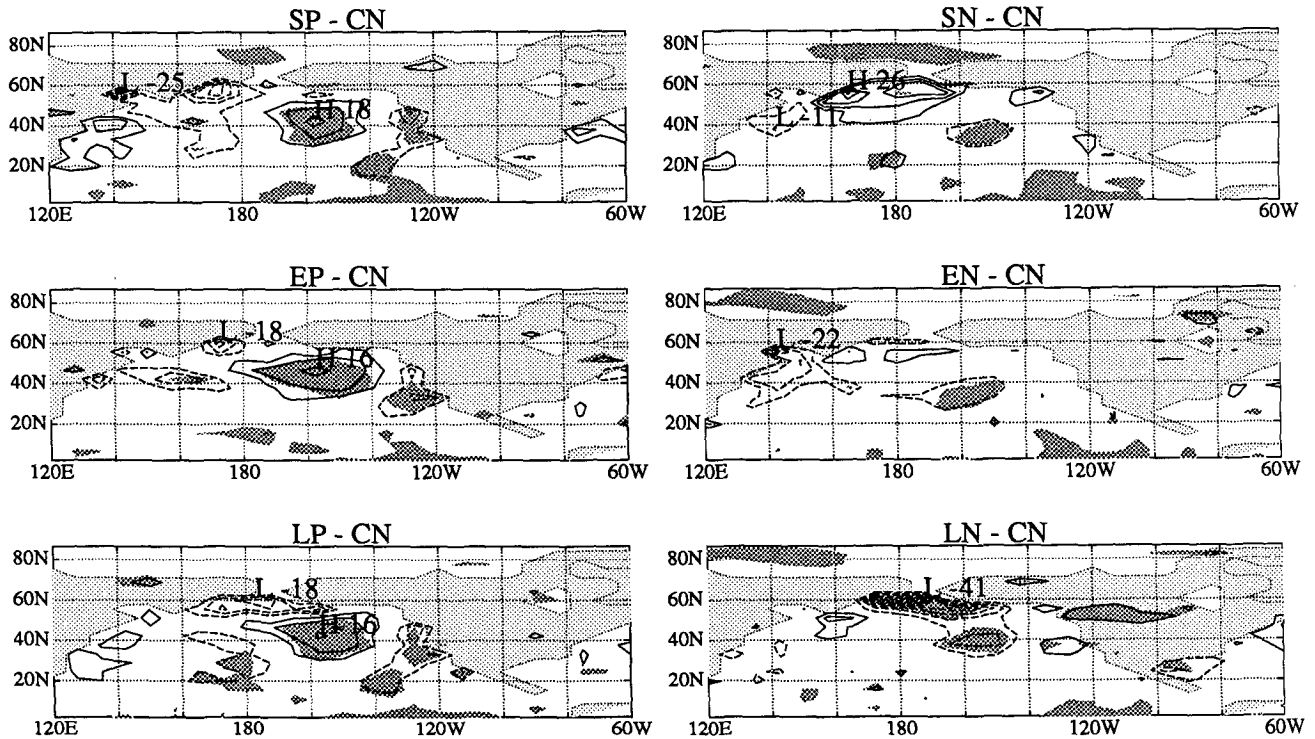
$H_s$ 

FIG. 8. As in Fig. 3, but for the response in the sensible heating field (vertically integrated heat diffusion). Contour interval is  $5 \text{ W m}^{-2}$ ; zero contour is omitted.

on the unrealistically vigorous baroclinic activity there. In contrast, the imposition of a stronger thermal gradient when a positive anomaly is prescribed may not be able to further intensify the already intense eddy field. The relationship between the prescribed SST anomaly and the model's storm track raises another issue. It is possible that the model's response has been influenced by imposing an SST anomaly based on observations in a way that may not be entirely consistent with the difference between the model's climate and the real one.

In contrast to the variations in the eddy heat fluxes, the eddy momentum fluxes seem to change in the positive anomaly runs as well as in the negative runs. The relationship between the patterns of eddy momentum transport and the time-averaged response is always such that the eddy transports reinforce the anomalies in the time-averaged flow (Figs. 4 and 7). This is consistent with recent observational work by Lau (1988) and modeling experiments by Robinson (1990). Both studies suggest the existence of an inherent coupling between high- and low-frequency transients in the atmosphere. In the observational study, Lau showed that the quasi-stationary geopotential height tendency induced by eddy momentum fluxes is in phase with the height fluctuations in the monthly averaged circulation.

In the model study, Robinson found that the eddy vorticity fluxes tend to reinforce the low-frequency waves and retard their eastward propagation. A similar consistent relationship was noted by Palmer and Sun (1985) and Lau and Nath (1990).

In the present study, the initial response patterns were found to be different from the equilibrium response. In particular, the short run SN yielded a more faithful simulation of the observations and the inherently transient study of Lau and Nath (1990) than the long run LN. In that respect, it is interesting to note that subtle differences exist between the SN and the EN response patterns. These differences make the EN response more similar to the LN response. Further investigation is needed to confirm these subtle differences; however, these results may indicate that the atmospheric response to midlatitude SST anomalies entails a very slow process of adjustment, with time scales longer than a season or so. The reasons for such slow adjustment may lie in the interplay between baroclinic eddies and the quasi-stationary flow, which may define a time scale longer than that associated with the dispersion of long Rossby waves. Thus, our results indicate that the short runs may be more relevant to the understanding of seasonal ocean-atmosphere interactions than the long runs are. These aspects should be con-

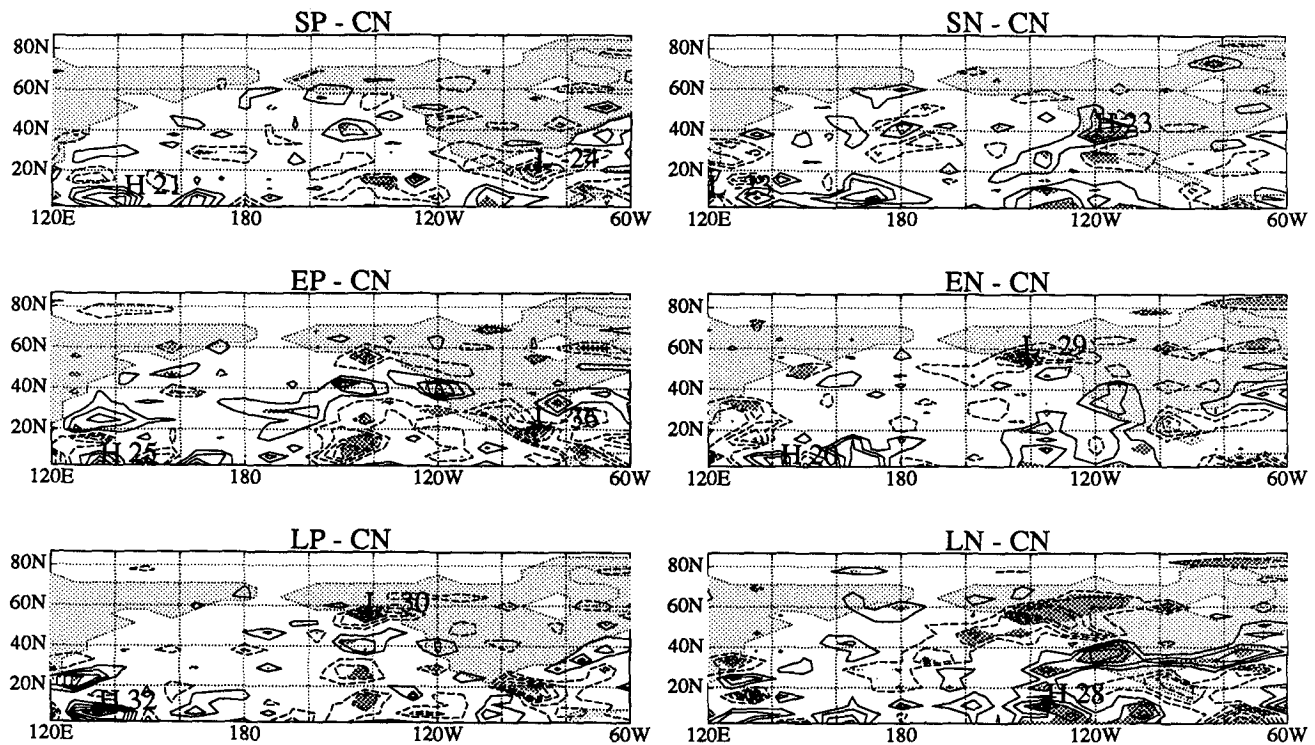
$H_q$ 

FIG. 9. As in Fig. 3, but for the vertically integrated condensational heating field. Contour interval is  $5 \text{ W m}^{-2}$ ; zero contour is omitted.

sidered carefully when developing strategies for future GCM simulations of climate variability.

**Acknowledgments.** We thank S. Manabe and the Climate Dynamics Project at GFDL for making the GCM available and providing the computer time for its integration. T. Broccoli, T. Delworth, and M. J. Nath extended generous help in integrating the GCM. Discussions with K. Cook, I. Held, C. Frankignoul, W. Robinson, M. Ting, and S. Zebiak were helpful and stimulating. I. Held and J. Lanzante offered useful comments on an earlier version of this manuscript. Model integrations and preliminary analysis of the results were conducted using the CDC Cyber 205 computer at GFDL, where the first author was supported by NOAA Grant NA 87EA-D-OA039. Additional analysis of the results at the Lamont-Doherty Geological Observatory was made possible through a generous gift of the G. Unger Vetelsen Foundation.

## REFERENCES

- Davis, R., 1976: Predictability of sea-level pressure anomalies over the North Pacific Ocean. *J. Phys. Oceanogr.*, **8**, 233–246.
- Frankignoul, C., 1985: Sea surface temperature anomalies, planetary waves, and air-sea feedback in middle latitudes. *Rev. Geophys.*, **23**, 357–390.
- Held, I. M., 1983: Stationary and quasi-stationary eddies in the extratropical troposphere: Theory. *Large Scale Dynamical Processes in the Atmosphere*, R. P. Pearce and B. J. Hoskins, Eds., Academic Press, 127–168.
- , and M. Ting, 1990: Orographic versus thermal forcing of stationary waves and the importance of the mean low-level wind. *J. Atmos. Sci.*, **47**, 495–500.
- Hendon, H. H., and D. L. Hartmann, 1982: Stationary waves on a sphere: Sensitivity to thermal feedback. *J. Atmos. Sci.*, **39**, 1906–1920.
- Hoskins, B. J., and D. Karoly, 1981: The steady linear response of a spherical atmosphere to thermal and orographic forcing. *J. Atmos. Sci.*, **38**, 1179–1196.
- Iwasaka, N., K. Hanawa, and Y. Toba, 1987: Analysis of SST anomalies in the North Pacific and their relation to 500 mb height anomalies over the Northern Hemisphere during 1969–1979. *J. Meteor. Soc. Japan*, **65**, 104–114.
- Lanzante, J. R., 1984: A rotated eigenanalysis of the correlation between 700-mb heights and sea surface temperatures in the Pacific and Atlantic. *Mon. Wea. Rev.*, **112**, 2270–2280.
- Lau, N.-C., 1988: Variability of the observed midlatitude storm tracks in relation to low-frequency changes in the circulation pattern. *J. Atmos. Sci.*, **45**, 2718–2743.
- , and M. J. Nath, 1987: Frequency dependence of the structure and temporal development of wintertime tropospheric fluctuations—comparison of a GCM simulation to observations. *Mon. Wea. Rev.*, **115**, 251–271.
- , and —, 1990: A general circulation model study of the atmospheric response to extratropical SST anomalies observed in 1950–1979. *J. Climate*, **3**, 965–989.
- Lorenz, E. N., 1979: Forced and free variations of weather and climate. *J. Atmos. Sci.*, **36**, 1367–1376.

- Morrison, D. F., 1976: *Multivariate Statistical Methods*. McGraw-Hill series in probability and statistics, 415 pp.
- Namias, J., 1959: Recent seasonal interactions between North Pacific waters and the overlying atmospheric circulation. *J. Geophys. Res.*, **64**, 631-646.
- , 1965: Short-period climatic fluctuations. *Science*, **147**, 696-706.
- , 1969: Seasonal interactions between the North Pacific Ocean and the atmosphere during the 1960s. *Mon. Wea. Rev.*, **97**, 173-192.
- , 1978: Multiple causes of the North American abnormal winter 1976-77. *Mon. Wea. Rev.*, **106**, 279-295.
- , 1979: *Northern Hemisphere Seasonal 700 mb Height and Anomaly Charts, 1947-1978, and Associated North Pacific Sea Surface Temperature Anomalies*. CALCOFI Atlas No. 27, State of California Marine Research Committee, 275 pp.
- , and D. R. Cayan, 1981: Large-scale air-sea interactions and short period climate fluctuations. *Science*, **214**, 869-876.
- Navarra, A., 1990: Steady, linear response to thermal forcing of an anomaly model with an asymmetric climatology. *J. Atmos. Sci.*, **47**, 148-169.
- Palmer, T. N., and Z. Sun, 1985: A modeling and observational study of the relationship between sea surface temperatures in the north west Atlantic and the atmospheric general circulation. *Quart. J. Roy. Meteor. Soc.*, **111**, 947-975.
- Pitcher, E. J., M. L. Blackmon, G. T. Bates, and S. Munoz, 1988: The effect of North Pacific sea surface temperature anomalies on the January climate of a general circulation model. *J. Atmos. Sci.*, **45**, 173-188.
- Robinson, W. A., 1990: The dynamics of low-frequency variability in a simple model of the global atmosphere. *J. Atmos. Sci.*, **48**, 429-441.
- Ting, M., 1991: The stationary wave response to a midlatitude SST anomaly in an idealized GCM. *J. Atmos. Sci.*, **48**, 1249-1275.
- Trenberth, K. E., and J. G. Olson, 1988: ECMWF Global Analyses 1979-1986: Circulation statistics and data evaluation. NCAR Tech. Note NCAR/TN-300+STR. 94 pp. plus 12 fiche.
- Valdez, P. J., and B. J. Hoskins, 1989: Linear stationary wave simulation of the time-mean flow. *J. Atmos. Sci.*, **46**, 2509-2527.
- Wallace, M. J., and D. S. Gutzler, 1981: Teleconnections in the geopotential height field during the Northern Hemisphere winter. *Mon. Wea. Rev.*, **109**, 784-812.
- , and Q. Jiang, 1987: On the observed structure of interannual variability of the atmosphere/ocean climate system. *Atmospheric and Oceanic Variability*, H. Cattle, Ed., Roy. Meteor. Soc., 17-43.
- , C. Smith and Q. Jiang, 1990: Spatial patterns of atmosphere-ocean interaction in the northern winter. *J. Climate*, **3**, 990-998.
- Weare, B., A. Navato and R. E. Newell, 1976: Empirical orthogonal analysis of Pacific Ocean sea surface temperatures. *J. Phys. Oceanogr.*, **6**, 671-678.